COMMUNICATION

ChemComm
www.rsc.org/chemcomm

Three-dimensional imaging of YB_{56} by high-resolution electron microscopy†

Takeo Oku
Institute of Scientific and Industrial Research, Osaka University, Mihogaoka 8-1, Ibaraki Osaka 567-0047, Japan. E-mail: oku@sanken.osaka-u.ac.jp

Received (in Cambridge, UK) 5th September 2001, Accepted 6th December 2001
First published as an Advance Article on the web 18th January 2002

The three-dimensional potential map of YB_{56} was obtained by inverse Fourier transformation of three-dimensional phases and amplitudes in three high-resolution images taken along the [100], [110] and [111] directions of YB_{56} crystals; the size of the imaging region was 14 nm × 14 nm × ~4 nm, and the image directly showed the three-dimensional potential map of the crystal, a useful method for three-dimensional structure analysis in nanoscale regions.

For soft X-ray synchrotrons in the 1–2 keV energy region, high-resolution and radiation resistant monochromators are required. Gadolinium gallium garnet and beryl are used for monochromators because of the *d*-spacing of these materials. However, the crystal quality of these materials is low, and they suffer from synchrotron radiation damage. Recently, high quality YB_{56} single crystals, with the YB_{66} structure,[1–3] have been synthesized for use as high-resolution and synchrotron radiation resistant monochromators.[4,5] After the discovery of the application of YB_{56} as a soft X-ray monochromator, the crystal structure of YB_{56} (a = 2.34600 nm) was determined using single crystal X-ray diffractometry.[6] The boron framework of YB_{56} is basically made of 8 super-icosahedra $(B_{12})_{13}$ and 8 non-icosahedral B_{80} clusters (total 1584 boron atoms). The site occupancy of yttrium in YB_{56} is 0.575, which suggests that the peanut-shaped 'Y-sites' (a pair of yttrium atoms) in the boron clusters should be occupied in most cases by only one yttrium atom.[2,3,6]

High-resolution electron microscopy (HREM) is a powerful method for direct observation of the atomic structure of advanced materials.[7–9] In previous works,[10,11] the Y-holes in YB_{56} were directly detected in the boron clusters by HREM, and the 'local' structure model was proposed for yttrium atom arrangements. In addition, a residual index ($R_{\mathrm{HREM}} = I_{\mathrm{obs}} - I_{\mathrm{calc}}/I_{\mathrm{obs}}$) was used for image analysis to determine the crystal thickness and defocus value of the observed images, and differential images showed the atomic disordering of the boron atoms around the Y-holes.[12,13] However, no observation has been reported yet on the three-dimensional potential distribution in YB_{56} crystals in the nanoscopic region.

The purpose of the present work is to obtain three-dimensional information for YB_{56} crystals with nanoscopic sizes by using high-resolution electron microscopy. In the present work, crystallographic image processing was applied for image analysis, which is expected to provide three-dimensional atomic positions. A slow-scan CCD camera with high linearity and electron sensitivity was used to record HREM images digitally.

High quality single crystals of YB_{56} were grown by an indirect heating floating-zone method.[4,5] The molten zone was heated by radiation from an inductively heated tungsten ring. The tungsten ring was placed between the work coil and the molten zone. A set of growth conditions for getting high quality YB_{56} single crystals is as follows: growth direction = [100], growth rate = 10 mm h^{-1}, rotation rate = 6 rpm (growth axis), atmosphere = He 0.3 MPa, composition of crystal [B]/[Y] = 56, and composition of the molten zone [B]/[Y] = 40.

Samples for HREM observation were prepared by dispersing crushed materials on holey carbon grids. HREM observations were performed with a 400 kV electron microscope (JEM-4000EX) having a resolution of 0.17 nm. The electron microscope is equipped with a slow-scan charge-coupled-device (CCD) camera (Gatan SSC model 694) and a LaB_6 cathode. The area of detection of the CCD camera is 1024 × 1024 pixels with a pixel size of 24 × 24 μm. For image processing of the observed HREM images, Digital Micrograph (Gatan Inc., CA, USA), TriView and CRISP (Calidris Corp., Stockholm, Sweden) software were used.

In order to get three-dimensional atomic arrangements, three-dimensional HREM observations were carried out. The [100], [110] and [111] directions of the YB_{56} crystals were selected in order to obtain the three-dimensional potential map of YB_{56}. Fig. 1(a)–(c) show HREM images of YB_{56} recorded along the [100], [110] and [111] directions, respectively, using the slow-scan CCD camera. The right sides of the 3 images are the thinnest regions of the YB_{56} crystals. To get optimal resolution (0.016 nm pixel^{-1}), the digital images were recorded at microscope magnifications of 1.0×10^6. The images were recorded close to the Scherzer defocus condition (−49 nm). Fourier transforms of Fig. 1(a)–(c) are shown in Fig. 1(d)–(f), respectively. Open circles indicate the resolution limit of the electron microscope of 0.17 nm.

In order to observe the potential distribution more clearly, crystallographic image processing was carried out on the Fourier transforms in Fig. 1. The reciprocal lattice was indexed, and the lattice distances were estimated using the positions of the strongest peaks in the transforms. The local background and reflections below the resolution limit (0.17 nm) were subtracted, and the amplitudes and phases of the peaks were determined. 46 Independent reflections were obtained from the 3 HREM images, as listed in Table S1 (ESI†). Before correcting the phases, the phase origin was determined by investigating the origin shift that gave the best accordance with the phase conditions for the two-dimensional space group. The effect of the contrast transfer function of the objective lens was corrected. The focus was determined by using residual indices between experimental and calculated HREM images. The corrected phases, refined by using crystallographic symmetrization,[14,15] based on the two-dimensional space group, were used for the reconstruction of the Fourier transforms.

Fig. 2(a) is a three-dimensional potential map reconstructed from three-dimensional phases and amplitudes from the Fourier transforms in Table S1.† The color shading is on an arbitrary scale for clear mapping. Fig. 2(b) is a perspective view of a structure model of YB_{56}. This three-dimensional potential map is different from conventional two-dimensional HREM images, and it shows the three-dimensional potential map of the crystal. The three-dimensional potential map of YB_{56} in Fig. 2(a) shows a complicated potential distribution, which is due to the complexity of the YB_{56} structure. Since the crystal thickness is thin enough (< ~5 nm) to satisfy the conditions of the weak-

---

† Electronic supplementary information (ESI) available: Table S1: three-dimensional amplitudes and symmetrized phases of YB_{56} in Fourier transform derived by crystallographic image processing of HREM images, and amplitudes obtained from electron diffraction patterns. See http://www.rsc.org/suppdata/cc/b1/b107864j/

DOI: 10.1039/b107864j

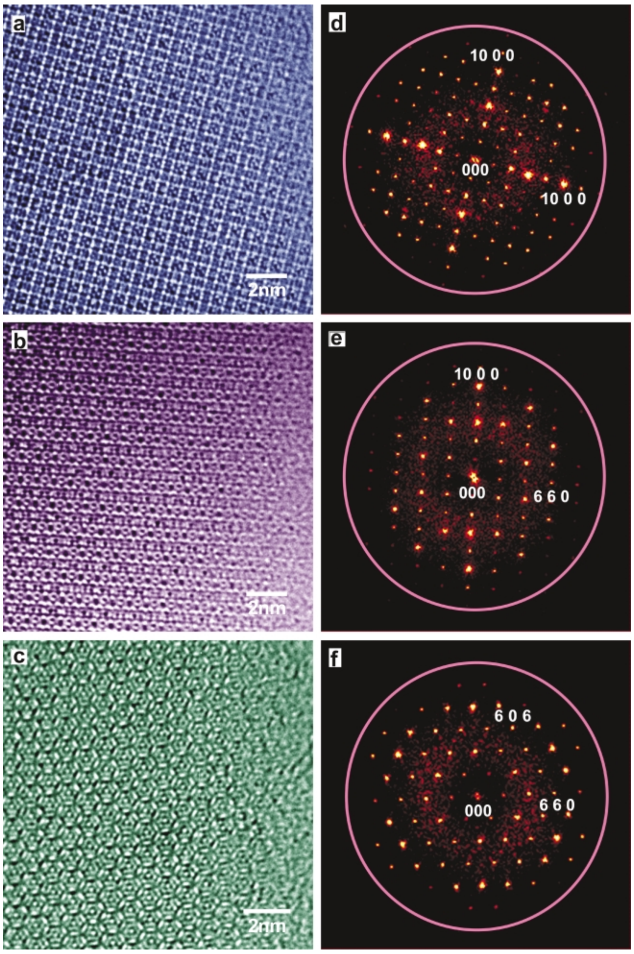

Fig. 1 HREM images of thin parts of the YB_{56} crystals taken along the (a) [100], (b) [110], and (c) [111] directions. (d), (e), (f) Fourier transforms of (a), (b), and (c), respectively. Open circles indicate the resolution limit of the electron microscope (0.17 nm).

phase objective approximation, the dynamical effect is weak, and the image directly shows the potential distribution in YB_{56}. The potential is high at the Y-atom positions, and low around the boron atoms in Fig. 2(a). However, the boron atom, which has a fairly low atomic number ($Z = 5$) compared to the yttrium atom ($Z = 39$), still shows the potential distribution in the observed three-dimensional potential map of YB_{56} [Fig. 2(a)].

Most of the structure determinations by HREM have been carried out based on two-dimensional data recorded along a short unit cell axis. The atomic positions along the short axis were estimated from geometries and chemical compositions. This two-dimensional method is not suitable for crystals with long unit cell axes, such as borides. Recently, pore structures in mesoporous materials were evaluated by a three-dimensional method,[16] and the porosity was directly estimated from three-dimensional images in mesoscale. In the present work, a full three-dimensional reconstruction in nanoscale was successfully carried out from HREM images taken along three crystallographic directions.

In conclusion, 46 independent phases and amplitudes were extracted from Fourier transforms of high-resolution images, which were taken along the [100], [110] and [111] directions under the conditions of the weak-phase objective approximation, of YB_{56} nanocrystals with a size of 14 nm × 14 nm × ∼4 nm. After revision of the contrast transfer function, inverse Fourier transformation was carried out, and the three-dimensional potential map of YB_{56} was obtained. The image directly showed the potential map of the YB_{56} crystal with ∼1600 atoms in the unit cell. The present work indicates that the three-dimensional potential map will be useful for three-dimensional structure analysis in the nanoscale region of nanocrystal materials.

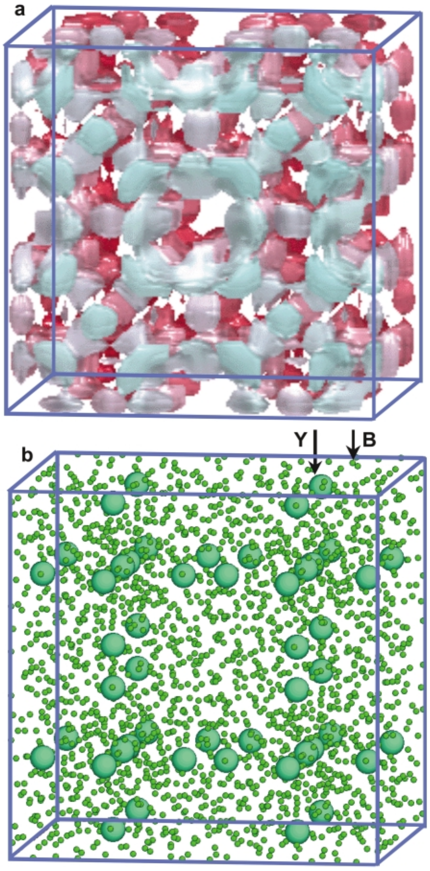

Fig. 2 (a) Three-dimensional potential map of YB_{56} obtained by inverse Fourier transformation of three-dimensional phases and amplitudes. (b) Perspective view of YB_{56}.

The author would like to acknowledge Professors J.-O. Bovin, I. Higashi, T. Tanaka, S. Hovmöller and X.-D. Zou for useful discussion and providing samples.

Notes and references

1 A. U. Seybolt, *Trans. Am. Soc. Met.*, 1960, **52**, 971.
2 S. M. Richards and J. S. Kasper, *Acta Crystallogr.*, 1969, **25**, 237.
3 G. A. Slack, D. W. Oliver, G. D. Brower and J. D. Young, *J. Phys. Chem. Solids*, 1977, **38**, 45.
4 K. Kamimura, T. Tanaka, S. Otani, Y. Ishizawa, Z. U. Rek and J. Wong, *J. Cryst. Growth*, 1993, **128**, 429.
5 T. Oku and I. Higashi, *Solid State Commun.*, 2000, **115**, 547; T. Oku, H. Kubota, T. Ohgami and K. Saganuma, *Carbon*, 1999, **37**, 1299.
6 I. Higashi, K. Kobayashi, T. Tanaka and Y. Ishizawa, *J. Solid State Chem.*, 1997, **133**, 16.
7 T. Oku and S. Nakajima, *Appl. Phys. Lett.*, 1999, **75**, 2226.
8 T. Oku, A. Carlsson, J.-O. Bovin, C. Svensson, L. R. Wallenberg, C. Linke and M. Jansen, *Acta Crystallogr., Sect. B*, 2000, **56**, 363.
9 T. Oku, *J. Ceram. Soc. Jpn.*, 2001, **109**, 17.
10 T. Oku, A. Carlsson, L. R. Wallenberg, J.-O. Malm, J.-O. Bovin, I. Higashi, T. Tanaka and Y. Ishizawa, *J. Solid State Chem.*, 1998, **135**, 182.
11 T. Oku, *J. Electron Microsc.*, 2000, **49**, 41.
12 T. Oku and J.-O. Bovin, *Philos. Mag. A*, 1999, **79**, 821.
13 T. Oku, J.-O. Bovin, I. Higashi, T. Tanaka and Y. Ishizawa, *J. Mater. Res.*, 2001, **16**, 101.
14 S. Hovmöller, A. Sjögren, G. Farrants, M. Sundberg and B.-O. Marinder, *Nature*, 1984, **331**, 238.
15 T. E. Weirich, R. Ramlau, A. Simon, S. Hovmöller and X. D. Zou, *Nature*, 1996, **382**, 144.
16 Y. Sakamoto, M. Kaneda, O. Terasaki, D. Y. Zhao, J. M. Kim, G. Stucky, H. J. Shin and R. Ryoo, *Nature*, 2000, **408**, 449.